

Hall effect of epitaxial $\text{YBa}_2\text{Cu}_3\text{O}_{7-x}$ and $\text{Bi}_2\text{Sr}_2\text{CaCu}_2\text{O}_y$ films: Interpretation of the Hall effect on the basis of a renormalized tight-binding model

R. Hopfengärtner, M. Leghissa, G. Kreiselmeyer, B. Holzapfel,* P. Schmitt,* and G. Saemann-Ischenko

Physikalisches Institut, Universität Erlangen-Nürnberg, Erwin-Rommel-Strasse 1, D-8520 Erlangen, Federal Republic of Germany

(Received 2 April 1992; revised manuscript received 10 July 1992)

The Hall effect of epitaxial $\text{YBa}_2\text{Cu}_3\text{O}_{7-x}$ ($T_c \approx 90$ K) and $\text{Bi}_2\text{Sr}_2\text{CaCu}_2\text{O}_y$ ($T_c \approx 80$ K) films has been investigated. In both compounds the Hall coefficient R_H ($B \parallel c$ axis) in the normal phase is positive and exhibits a strong temperature dependence, which is more pronounced in $\text{YBa}_2\text{Cu}_3\text{O}_{7-x}$ than in $\text{Bi}_2\text{Sr}_2\text{CaCu}_2\text{O}_y$. On the basis of a renormalized two-dimensional tight-binding band structure the normal-state Hall coefficient R_H has been calculated as a function of doping concentration and temperature using the relaxation-time approximation. Strong correlation effects are considered to some extent via doping-dependent nearest- and next-nearest-neighbor hopping terms leading to band-narrowing effects. The consideration of the latter term strongly influences the Hall coefficient. The Hall effect has been explored for two quite different models: (i) doping creates holes close to the top of an *effective* oxygen band, which is located between the lower and the upper Hubbard band; (ii) doping creates holes in a less than half-filled antibonding CuO_2 subband. The influence of the relaxation time $\tau(\mathbf{k})$ on the Hall coefficient has been explored by considering two simple choices, namely a \mathbf{k} -independent τ_0 , and $\tau(\mathbf{k}) = l(T, \delta)/|v(\mathbf{k})|$ (l is the mean free path and δ the doping concentration). Depending on the relaxation time different results have been obtained for the Hall coefficient. Assuming that holes are doped in the oxygen band and $\tau(\mathbf{k}) \propto |v(\mathbf{k})|^{-1}$ a good agreement between theory and experimental data of $\text{Bi}_2\text{Sr}_2\text{CaCu}_2\text{O}_y$ has been achieved, whereas for $\text{YBa}_2\text{Cu}_3\text{O}_{7-x}$ the pronounced temperature dependence of R_H is qualitatively reproduced. A comparison between the predictions of the Hall effect and the corresponding Fermi surfaces is made. We have also calculated some band parameters including the Drude plasma energy, the Fermi velocity, and the carrier effective mass.

I. INTRODUCTION

Besides their high T_c 's and striking superconducting features the cuprate superconductors exhibit a large number of anomalous normal-state properties, which seem to be a hallmark of them. An understanding of these unusual properties in the normal phase may provide some clues for the mechanism of superconductivity. Among various other transport phenomena the Hall effect is considered to be a very important quantity that provides valuable information about the electronic structure of the high- T_c superconductors (HTSC) in the normal state. Recently, the Hall effect has stimulated immense efforts of both experimental and theoretical investigations.¹ While on the experimental side a consolidation of results for different families of HTSC has been achieved, there is up to now no commonly accepted consensus about the theoretical interpretation of the normal-state Hall effect. Investigations on the Hall coefficient of the $\text{La}_{2-x}\text{Sr}_x\text{CuO}_4$ compound² suggest that R_H varies as $1/x$ in the small doping regime. Results of a conventional band-structure calculation³ predict a doping dependence of the Hall coefficient, which is not compatible with experiment. Based on this and other observations, it has been claimed that Fermi-liquid theory for the normal state is not adequate. Concerning the Hall effect for small x strongly correlated models (e.g., Ref. 4) are more promising. On the other hand, if the doping is large, angle-resolved photoemission spectroscopy measurements⁵⁻⁷ (ARPES) in some of

the copper-oxide superconductors indicate a large Fermi surface, which in turn seems to be consistent with band-structure calculations.⁸ Opposed to this experimental fact, some of the strongly correlated models predict very different shapes of the Fermi surface. This is especially true for small doping concentrations. Therefore, it appears that these two types of experiments provide conflicting information about the electronic structure in the normal state. Moreover, high- T_c superconductors reveal an unusual temperature dependence of the Hall effect, which is also a very puzzling phenomenon.

In this paper the Hall coefficient in the normal phase is investigated both experimentally and theoretically. We report a comparative study of Hall effect measurements carried out on several epitaxial $\text{YBa}_2\text{Cu}_3\text{O}_{7-x}$ and $\text{Bi}_2\text{Sr}_2\text{CaCu}_2\text{O}_y$ films, which have been prepared by pulsed laser ablation. The Hall coefficient has been calculated within the framework of a renormalized two-dimensional (2D) tight-binding model on a square lattice, which might be a reasonable starting point for cuprates in the regime of high doping concentrations. Our approach is based on the conventional Boltzmann transport equations, i.e., the relaxation-time approximation. Here we focus our discussion to both the doping as well as the temperature dependence of the normal-state Hall coefficient. Due to the lack of a precise knowledge about the relaxation time $\tau(\mathbf{k})$ describing the complicated scattering processes in the HTSC we have investigated two simple approaches for it. As will be discussed in detail below, the choice of $\tau(\mathbf{k})$ as well as the consideration of the

next-nearest-neighbor hopping term in the tight-binding model strongly influence the predicted Hall coefficient. The interpretation of the Hall effect has been made for two different models. In the first model the tight-binding dispersion describes an effective oxygen band, in which the doped holes are introduced close to the top of the upper band edge. In the second model we assume that additionally doped holes are created in the antibonding CuO_2 band. In this case the band is less than half filled. The Hall coefficient has been calculated for various parameter sets and is compared to experimental data. The difficulties and problems that arise with respect to the interpretation of the Hall effect and the corresponding shapes of the Fermi surfaces for the two different models are outlined. Finally, we briefly discuss some calculated band parameters.

This paper is organized as follows. In Sec. II we introduce our model for the electronic structure of the CuO_2 planes. A brief review of the formalism is given, which is used for the calculation of the Hall effect. Here also some theoretical results on the doping and temperature dependence of the Hall coefficient are discussed. Section III deals with the experimental details of the measurements. In Sec. IV we present experimental data and compare them to theory. In Sec. V we summarize our results.

II. THEORY

A. Electronic structure of the metallic phase

It is widely accepted that the electronic structure of the HTSC is dominated by the quasi-two-dimensional CuO_2 planes where strong correlation effects in the $\text{Cu } 3d$ orbitals play a crucial role. Depending on the hole doping concentration δ (here we restrict our discussion to the hole-doped cuprates), high- T_c superconductors evolve from an antiferromagnetic insulator for very small δ to a metallic phase, in which the superconducting phase transition takes place, for larger values of the hole doping. Much of the theoretical efforts have focused on strongly correlated models such as the large- U one-band Hubbard model,⁹ the t - J model,¹⁰ the multiband Hubbard model,¹¹ or the Anderson lattice Hamiltonian,¹² etc. These models are very promising for an understanding of the nature of the electronic states in the small doping limit that is, near the charge transfer or Mott-Hubbard transition, respectively. Presumably, an increase of the hole-doping concentration gradually reduces the dominance of strong correlation effects. Currently a central issue is whether or not strong correlations are still present in the heavily doped systems. In this doping regime the predictions of the conventional band-structure calculations⁸ seem to describe the electronic structure near the Fermi energy quite well. In this paper our goal is to calculate the normal-state Hall coefficient $R_H(T, \delta)$ on the basis of a simple model. We propose for the quasi-2D electronic structure of the HTSC the following tight-binding energy-dispersion relation:

$$\begin{aligned} \epsilon(\mathbf{k}) = & -2\tilde{t}[\cos(k_x a) + \cos(k_y a)] \\ & -4\tilde{t}^* \cos(k_x a) \cos(k_y a), \end{aligned} \quad (1)$$

where

$$\tilde{t} = t\delta, \quad \tilde{t}^* = t^*\delta \quad (2)$$

denote the renormalized nearest- and next-nearest-neighbor hopping terms, δ the doping concentration (per site), and a the lattice constant. Strong correlation effects are accounted for by means of more or less phenomenologically introduced renormalization factors in the hopping terms, which lead to band narrowing. The renormalization factors have been adopted from early calculations on the large- U one-band Hubbard model,¹³ where the constraint of *no* doubly occupied sites is approximated on the mean-field level resulting in the renormalized nearest-neighbor transfer term \tilde{t} . Additionally, for the next-nearest-neighbor hopping term t^* we assume the same renormalization. It is worth noting that there is a close resemblance of the dispersion (1) to the resulting Cu-fermion quasiparticle band,¹⁴ which have been derived from the three-band CuO_2 model using the $U_d = \infty$ mean-field slave-boson approach. Here the effective hopping terms are essentially functions of the bare parameters t_{pd} , t_{pp} , E_d , E_p and the doping concentration δ . t_{pd} is the Cu-O hopping, t_{pp} the direct O-O transfer term, and E_d, E_p are the atomic levels on Cu and O, respectively. In our study we treat both transfer integrals as free parameters, i.e., $t > 0$, while t^* takes positive or negative values. Of course our model, which also completely neglects the three-dimensional coupling of the CuO_2 planes, is certainly a strong simplification of the electronic structure of high- T_c superconductors. Nevertheless, we believe that the essential ingredients of the nature of the electronic states in the large doping regime, far above the metal-insulator transition, are considered. A similar tight-binding band with fixed transfer terms has been proposed in Ref. 15. On the basis of the more familiar tight-binding scheme with $t^* = 0$ the superconducting transition temperature T_c has been calculated assuming that the Fermi energy is located very close to or exactly at the van Hove singularity.¹⁶

In the following we examine two quite different models to interpret the energy dispersion (1) for the HTSC. In the first approach the band structure describes a band, which we term for the sake of descriptiveness an effective oxygen band. This band is located between the lower and the upper Hubbard subbands. For small values of the hole doping concentration δ the Fermi energy is located close to the upper band edge, i.e., the band contains $2 - \delta$ electrons per site [see Fig. 1 (a)]. We want to emphasize that this simple picture must not be taken too literally, because the $\text{Cu } 3d$ orbitals complicate the situation. In the second case the band structure is related to an antibonding CuO_2 subband [Fig. 1 (b)] resulting from the hybridization of the $d_{x^2-y^2}$ copper orbital with the neighboring p_x and p_y oxygen orbitals as well as from direct oxygen-oxygen hopping processes. Here the band is less than half filled for $\delta > 0$. It should be mentioned that the latter interpretation is closely related to the results found by band-structure calculations. We shall not pay too much attention to the correct assignment of the above dispersion to the two approaches.

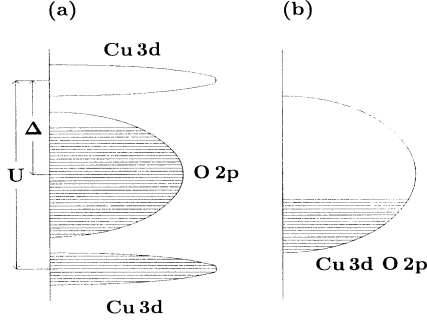


FIG. 1. Schematic plot of the band structure for doped CuO_2 planes. (a) Diagram illustrates the case where doped holes are induced in the O 2p band, which is located between the splitted Cu 3d bands. U denotes the on-site Coulomb interaction and Δ is the charge-transfer energy. (b) Band picture for a less than half-filled antibonding CuO_2 band.

In our study it is more important to concentrate on the different assumptions about the band filling. In Fig. 2 the density of states (DOS) $N(E)$ of the dispersion (1) is plotted for typical parameters, which below are also taken for numerical calculations of the Hall effect. The characteristic 2D van Hove singularity is apparent. For $t > 2|t^*|$ the logarithmic singularity in the DOS is due to the saddle points at $(k_x, k_y) = (0, \pm\pi a)$ and $(\pm\pi a, 0)$. One may ask whether such a singularity in the DOS can be observed experimentally (e.g., by photoemission spectroscopy) and furthermore, whether the sharp peak will still be preserved if an interplane coupling is introduced. These interesting questions cannot be discussed in detail in the present study. Here, we briefly point out the following: It is generally assumed that any interlayer coupling mechanism will broaden the singularity. But, as has recently been pointed out by Markiewicz,¹⁷ there are some forms of interlayer coupling, which have no effect at all on the van Hove singularity. Of course a finite transfer term t_z between neighboring planes, which causes an energy dispersion along the z direction, certainly influences the DOS. Depending on the magnitude of t_z the logarithmically divergent van Hove singularity of the exact two-dimensional system will be more or less smeared out. In this context the reader is referred to Ref. 18, in which the role of the van Hove singularity on T_c and on some normal-state properties in HTSC is pointed out. Moreover, it should be noted that the sharp peak in the DOS can also easily be smeared out by various structural defects.

Regardless of whether there is a diverging or a broadened van Hove singularity in the DOS already at this stage, the thermal broadening $(-\partial f/\partial E)$ of the Fermi

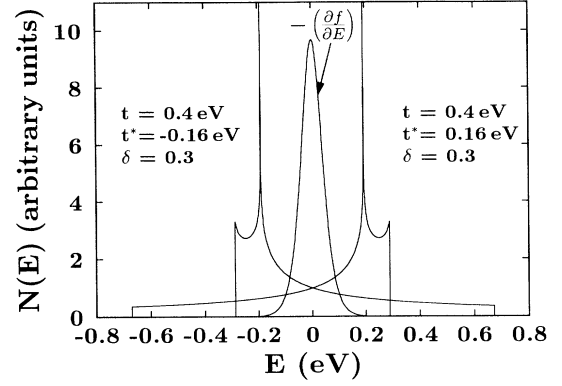


FIG. 2. Density of states $N(E)$ vs energy. The van Hove singularity occurs at $E = 4t^*\delta = \pm 0.192$ eV. Additionally shown is the derivative of the Fermi distribution function at $T = 300$ K, where a chemical potential of $\mu = 0$ eV has been chosen.

distribution function (Fig. 2), which is considerable on the scale of the bandwidth (of the order of 1 eV), indicates a strong influence of the temperature on transport properties.

B. Hall coefficient in the relaxation-time approximation

Whether the normal state of the HTSC can be described by a more or less conventional Fermi liquid (FL), a marginal FL,¹⁹ or not a FL at all,²⁰ is currently a central topic of discussion. A comparison between different Fermi-liquid schemes and their applicability to normal-state properties of HTSC can be found in the review article of Levin *et al.*²¹ On the basis of the Boltzmann transport theory, more precisely using the relaxation-time approximation, we try to interpret the doping and temperature dependence of the Hall coefficient. In this approach R_H is derived from an expression, which involves first and second derivatives of the energy dispersion. Thus, for a band structure like that of Eq. (1) the Hall number $n_H = (eR_H)^{-1}$ is, in general, *not* simply related to the real carrier concentration n . Moreover, the sign of R_H at $T = 0$ K, i.e., whether it is electronlike ($R_H < 0$) or holelike ($R_H > 0$), is essentially determined by the curvature of the Fermi surface. The Hall coefficient in the weak field limit, which corresponds also to our experimental set-up, is given by

$$R_H = R_{xyz}^H = E_y / (j_x B_z) = \sigma_{xyz} / (\sigma_{xx} \sigma_{yy}). \quad (3)$$

The formulae for the transport coefficients are:²²

$$\sigma_{xyz} = -\frac{2e^3}{\hbar V} \sum_{\mathbf{k}} \tau^2(\mathbf{k}) v_x(\mathbf{k}) \left(v_x(\mathbf{k}) \frac{\partial v_y(\mathbf{k})}{\partial k_y} - v_y(\mathbf{k}) \frac{\partial v_x(\mathbf{k})}{\partial k_x} \right) \left(-\frac{\partial f}{\partial \epsilon(\mathbf{k})} \right), \quad (4)$$

$$\sigma_{xx} = \sigma_{yy} = \frac{2e^2}{V} \sum_{\mathbf{k}} \tau(\mathbf{k}) v_x^2(\mathbf{k}) \left(-\frac{\partial f}{\partial \epsilon(\mathbf{k})} \right), \quad (5)$$

where V is the normalization volume, $\tau(\mathbf{k})$ denotes the relaxation time, $\hbar v_\alpha(\mathbf{k}) = \partial\epsilon/\partial k_\alpha$ ($\alpha = x, y$), and $f = \{\exp[(\epsilon - \mu(T, \delta))/k_B T] + 1\}^{-1}$ is the Fermi distribution function. In order to obtain some insights on the influence of the relaxation time $\tau(\mathbf{k})$, which, in general, might be a very complicated function, on the Hall coefficient, we examine two simple approaches for it:

$$\tau(\mathbf{k}) = \tau(T, \delta) = \tau_0, \quad (6)$$

$$\tau(\mathbf{k}) = \frac{l(\mathbf{k})}{|v(\mathbf{k})|} = \frac{l(T, \delta)}{\sqrt{v_x^2(\mathbf{k}) + v_y^2(\mathbf{k})}} = \tau_l. \quad (7)$$

The choice of a \mathbf{k} -independent τ_0 has *no* influence on R_H , while in the second case there is certainly one. In the formula for τ_l an anisotropic scattering of electrons might be partly reflected. In the following the \mathbf{k} -dependent relaxation time τ_l will be termed as constant- l relaxation time. Note, that the mean-free path $l(T, \delta)$ cancels out in expression (3). Therefore, the origin of a possible temperature dependence of the Hall coefficient in our model only comes from the Fermi distribution function. In the present study we do not address the unusual T linearity of the in-plane resistivity, which requires a detailed knowledge of the relaxation time. The evaluation of the Hall coefficient $R_H(T, \delta)$ has been performed numerically for $t > 2 |t^*|$ using standard methods to convert the 2D \mathbf{k} summation into an integration over constant energy surfaces. The temperature dependence of the chemical potential $\mu(T, \delta)$ has been taken into account. This quantity has been determined numerically for a given value of T and δ from the average number of electrons per site

$$n = \frac{2}{N} \sum_{\mathbf{k}} \frac{1}{\exp\{[\epsilon - \mu(T, \delta)]/k_B T\} + 1}, \quad (8)$$

where N is the number of sites. In the case of the oxygen band n is given by $2 - \delta$, while for the antibonding CuO_2 subband it corresponds to $n = 1 - \delta$. In the following we discuss some theoretical results of the doping and temperature dependence of the Hall coefficient.

C. Theoretical results of $R_H(\delta)$ at $T = 0$ K

In Figs. 3(a) and 3(b) we show the normalized Hall coefficient $R_H e / \tilde{V}_0$ (\tilde{V}_0 is the volume of the unit cell in the model) as function of the hole doping δ for different ratios t/t^* at $T = 0$ K. It should be stressed that the Hall coefficient $R_H(\delta, T = 0)$ depends only on the ratio t/t^* . This does not longer hold for finite T .

1. Results for the constant relaxation time τ_0

Examining the oxygen band [Fig. 3(a)] a negative value $t/t^* = -3$ leads to a positive Hall coefficient in the whole doping range of interest. The calculated $R_H(\delta)$ can be nicely fitted by the formula for free electrons (holes). A variation of t/t^* , supposed that the ratio remains negative, does not alter the predicted R_H -curve in the relevant doping range. For these hopping parameters the corresponding Fermi energy E_F is far above the van Hove

singularity. Thus the magnitude of $R_H(\delta)$ is essentially determined by the enclosed Fermi surface volume yielding this simple result. In contrast to the previous case a strongly decreasing Hall coefficient has been found for a positive value $t/t^* = 2.5$. In the small doping regime $R_H(\delta)$ is proportional to δ^{-1} , while for larger δ a pronounced deviation from the free-electron behavior can be seen including a sign change of R_H at $\delta = \delta_c \approx 0.38$. This critical doping concentration δ_c depends sensitively on the choice of the parameters t and t^* . The larger the value t/t^* the higher δ_c . For completeness we note that in the usual tight-binding band ($t^* = 0$) the Hall coefficient changes sign at $\delta = 1.0$. It should be pointed out that a similar strong variation of the Hall coefficient as function of the doping concentration including a sign reversal has been observed experimentally in $\text{La}_{2-x}\text{Sr}_x\text{CuO}_4$.² In this compound the hole doping concentration δ is, in a rather wide doping regime, identical to the Sr concentration x . Despite the qualitatively good agreement between theory and experiment one should keep in mind that our simple model is presumably not applicable in the small doping regime.

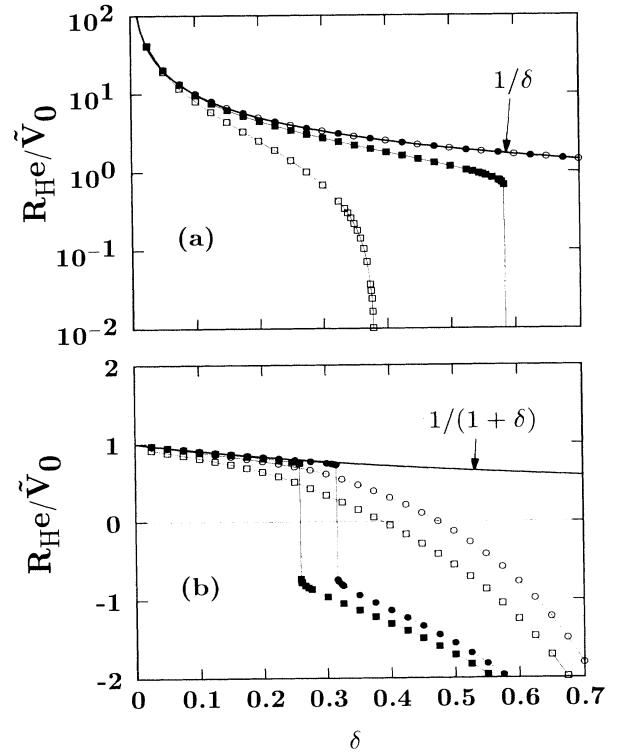


FIG. 3. Normalized Hall coefficient vs doping concentration δ at $T = 0$ K. The curves labeled by the open symbols have been calculated for τ_0 , while the solid symbols are the results assuming the constant- l relaxation time. The thin solid lines are guides for the eyes. Thick solid lines illustrate the result for the free-electron (hole) gas. (a) Doping creates holes in the $\text{O}2p$ band. The parameters are $t/t^* = -3.0$ (open and solid circles) and $t/t^* = 2.5$ (open and solid squares). (b) Doping induces holes in the antibonding CuO_2 band. The parameters are $t/t^* = -3.0$ (open and solid circles) and $t/t^* = -3.5$ (open and solid squares). Note the logarithmic scale in (a).

Concerning the results on the CuO_2 subband [Fig. 3(b)], there is also a pronounced dependence of $R_H(\delta)$ on δ . For the ratio $t/t^* = -3$ the Hall coefficient in the small doping regime is nearly the same as that of the free-electron gas [but now $\propto (1 + \delta)^{-1}$], while for larger δ a significant deviation is seen including a sign reversal of R_H at $\delta_c \approx 0.47$. Once more the critical doping concentration can be sensitively varied by the hopping parameters t and t^* . Concerning the prediction of the Hall coefficient for $t/t^* = -3.5$ there is already for very small δ a slight deviation from the $(1 + \delta)^{-1}$ behavior. In this case the corresponding Fermi energies are close to the van Hove singularity. For positive values of the ratio t/t^* and $\delta > 0$ the Hall coefficient is always *negative* (not shown here).

2. Results for the k -dependent relaxation time τ_l

In contrast to the results found for τ_0 , the choice of the constant- l relaxation time τ_l leads to some characteristically different predictions of the Hall coefficient. Assuming that excess holes are introduced in the oxygen band the ratio $t/t^* = -3$ yields the same behavior of R_H as in the case of τ_0 . For the ratio $t/t^* = 2.5$ the Hall coefficient is in a wide range a slowly decreasing function of δ . However, close to $\delta_c = 0.58$, which is significantly larger than the corresponding value found for the constant relaxation time τ_0 , R_H abruptly varies in magnitude followed by a sign change.

In the case of the CuO_2 band the overall behavior is very similar. It should be noted that for τ_l the sign change of R_H occurs exactly when the Fermi energy passes through the van Hove singularity. In general, this is not the case for τ_0 (with the exception $t^* = 0$). The origin of these pronounced differences of the Hall coefficient is essentially due to the strong influence of the k dependence of the relaxation time on the transport coefficient (4). Despite the fact that the particular choice of τ_l is phenomenological the results clearly illustrate the sensitivity of the Hall coefficient on the relaxation time.

D. Theoretical results of R_H at finite temperatures

Now we turn our attention to the temperature dependence of the Hall coefficient within our tight-binding model. In Figs. 4(a) and 4(b) we plot the normalized Hall coefficient as function of T , which is also accessible experimentally, for fixed hopping parameters varying the doping concentration δ . The bandwidths ($W = 8t\delta$) of the oxygen and the CuO_2 band range from 0.48 eV ($\delta = 0.2$) to 0.84 eV ($\delta = 0.35$) for the choice $t = 0.3$ eV, $t^* = 0.075$ eV, and from 0.64 eV ($\delta = 0.2$) to 1.12 eV ($\delta = 0.35$) for $t = 0.4$ eV, $t^* = -0.16$ eV, respectively. In both cases a considerable temperature dependence of R_H is seen. We would like to stress again that this comes solely from the temperature dependence of the Fermi distribution function. At first glance the strong dependence of R_H on T seems surprising, but is essentially a result of the small bandwidths of the order of 0.5–1.0 eV. This characteristic feature has to be combined with the fact

that the thermal broadening ($-\partial f/\partial E$) of the Fermi distribution function (see also Fig. 2), which enters in the formulae for R_H , is considerable (even for moderate T) on the scale of the corresponding bandwidths. Therefore, also such areas of constant energies in k space, which are not located in the immediate vicinity of the Fermi surface and which may have very different curvatures, contribute to the Hall coefficient resulting in the pronounced temperature dependence of it. Depending on the location of the chemical potential μ in the tight-binding band (and of course on T) it is possible that even both the holelike and electronlike orbits in the Brillouin zone contribute to R_H . This is especially true when μ is close to the van Hove singularity.

Besides the apparent differences in the magnitude of the Hall coefficient at $T \approx 0$ K for both doping cases, there is also a strong influence of the choice of the relaxation time on the detailed behavior of the $R_H(T)$ curves. Moreover, $R_H(T)$ is also dependent on t and t^* . In the case of the oxygen band the Hall coefficient varies more rapidly with increasing temperature for τ_0 than for τ_l . In the former, R_H is a decreasing function of T , while in the latter it increases first in the low-temperature regime

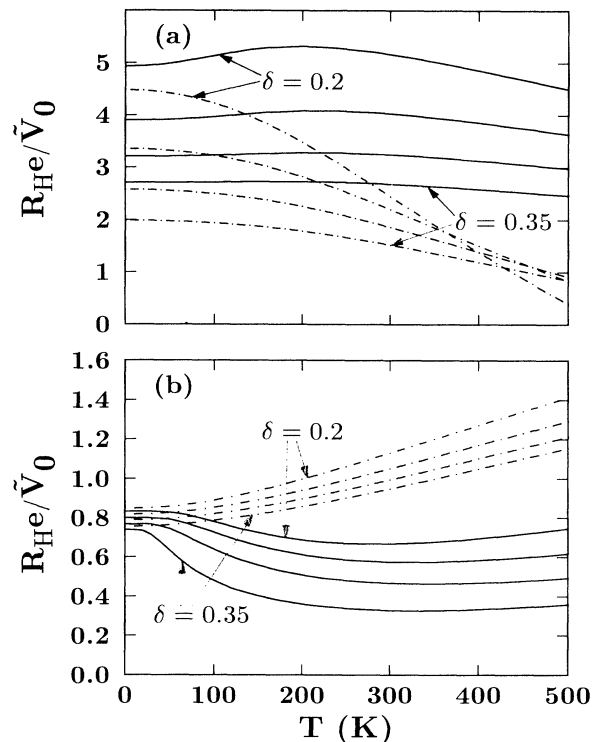


FIG. 4. Normalized Hall coefficient vs temperature for fixed transfer terms varying the doping concentration δ . The dot-dashed curves are the results for τ_0 and the solid lines are for τ_l . (a) Doping creates holes in the O $2p$ band. The parameters are $t = 0.3$ eV, $t^* = 0.075$ eV, and $\delta = 0.2, 0.25, 0.3, 0.35$ (on the left-hand side from top to bottom). (b) Doping induces holes in the antibonding CuO_2 band. The chosen parameters are $t = 0.4$ eV, $t^* = -0.16$ eV, and $\delta = 0.2, 0.25, 0.3, 0.35$ (also from top to bottom).

before it slightly decreases at higher temperatures. It should be pointed out, that for negative values of t^* and for the relevant doping concentrations, say $0 < \delta < 0.5$, the calculated Hall coefficient is essentially an increasing or nearly constant function of T for both relaxation time approaches (t and t^* are comparable to the above ones). Assuming that doping creates holes in the CuO_2 subband and a constant relaxation time, the Hall coefficient increases monotonically with increasing temperature, while for the constant- l relaxation time and the same parameters R_H is first a decreasing function of T before it slowly increases at higher temperatures. In general, the temperature dependence of R_H gradually becomes less pronounced by increasing the hole-doping concentration δ . The results illustrate that even within a simple one-band model a strong temperature dependence of the Hall coefficient is predicted, whose detailed behavior depends sensitively on the choice of the relaxation time and on the transfer terms t and t^* .

III. EXPERIMENTAL METHOD

In the present study epitaxial thin films of $\text{YBa}_2\text{Cu}_3\text{O}_{7-x}$ and $\text{Bi}_2\text{Sr}_2\text{CaCu}_2\text{O}_y$ (hereafter 1:2:3 and 2:2:1:2) were investigated. Both types of films were prepared by pulsed laser ablation onto (100) SrTiO_3 substrates. The details of the preparation procedure are described in Refs. 23 and 24. Several studies have been already reported on these 1:2:3 and 2:2:1:2 including e.g., anisotropic critical currents,^{25,26} normal-state transport properties,²⁷ influence of irradiation effects,²⁸ infrared reflectivity (FIR),²⁹ high-frequency conductivity,³⁰ and conversion-electron Mössbauer spectroscopy (CEMS).³¹

In the case of 1:2:3 the Hall bar has been patterned by photolithography and wet etching, while for the 2:2:1:2 samples it has been shaped mechanically. The transport measurements were carried out by a standard dc method. The temperature was measured by a platinum resistance thermometer. Typically, the sample current densities were in the range of 100–500 A/cm^2 for resistive, and $\approx 5000 \text{ A}/\text{cm}^2$ for Hall effect measurements. The Hall voltage for the configuration $B \parallel c$ axis ($j \parallel ab$ plane) was measured at fixed magnetic fields up to 5 T, while slowly sweeping the temperature. The signal due to the misalignment of the Hall contacts was eliminated by applying the magnetic field in two orientations perpendicular to the film surface.

IV. RESULTS AND DISCUSSION

A. Experimental results

The temperature dependence of the in-plane resistivity ρ of the samples, which are used in the Hall effect measurements, are shown in Figs. 5 (a) and 5(b). The superconducting transition temperatures T_c of the 1:2:3 samples are in the range of 88–90 K (zero resistance, see also Table I where some parameters are listed). The resistivity in the normal state is linear in T . However, a closer look at the 1:2:3 curves reveals a slight upward curvature

in the high-temperature regime. The extrapolated resistivity curves intercept close to zero residual resistivity at $T = 0 \text{ K}$. The rounding of the resistivity above T_c has been attributed to superconducting fluctuations.³² The 2:2:1:2 films have a $T_c \approx 80 \text{ K}$ and exhibit also a linear- T behavior far above T_c without any deviation from linearity at higher temperatures.

The Hall coefficients versus temperature of the 1:2:3 and 2:2:1:2 samples are shown in Figs. 6 and 7. The normal-state Hall coefficient in all samples is holelike and strongly depending on temperature. The Hall coefficient increases as the temperature is reduced, showing a maximum slightly above T_c , before it decreases at lower temperatures. In the superconducting phase transition the Hall coefficient exhibits a peculiar behavior including a sign reversal, which will be discussed in more detail in a forthcoming paper. The temperature dependence of R_H is stronger in 1:2:3 than in 2:2:1:2. The overall features of the Hall coefficient are in good agreement with reported data on high-quality 1:2:3 (Refs. 33 and 34) and 2:2:1:2 Ref. 35 samples (for a comprehensive overview about the Hall coefficient in HTSC see also Ref. 1). In this context it is worth noting that the temperature dependence of the normal-state Hall coefficient of high-quality single crystals is slightly more pronounced than in our epitaxial films. Presumably, this fact can be attributed to the lower concentration of structural defects in single crystals. In the case of 1:2:3 the reciprocal Hall coefficient can be approximated by $R_H^{-1}(T) = a(T + T_0)$ in the temperature range of 130 K up to about 200 K, while at higher temperatures a significant deviation is observed. Recently, this behavior was also observed in $\text{YBa}_2\text{Cu}_3\text{O}_{7-x}$ single crystals.³⁶ The deviation from lin-

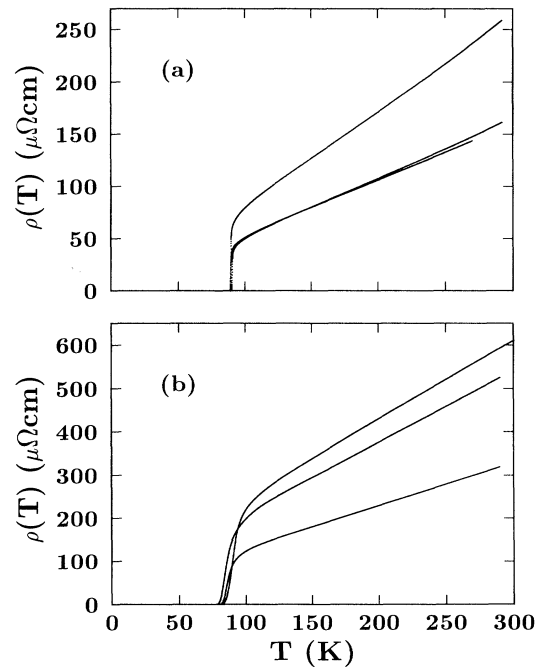


FIG. 5. Temperature dependence of the resistivity of the 1:2:3 (a) and of the 2:2:1:2 (b) samples.

TABLE I. Properties of the $\text{YBa}_2\text{Cu}_3\text{O}_{7-x}$ and $\text{Bi}_2\text{Sr}_2\text{CaCu}_2\text{O}_y$ films.

Compound	Sample	T_c (K)	$\rho(100\text{ K})$ ($\mu\Omega\text{ cm}$)	a ($\text{C}/\text{cm}^3\text{ K}$)	T_0 (K)	n_H^* (100 K)	n_H^* (250 K)
1:2:3	1	89.9	49.9	8.18	12.1	0.53	1.13
	2	88.5	51.2	8.99	17.2	0.61	1.28
	3	88.9	79.5	5.28	17.6	0.36	0.75
2:2:1:2	1	80.0	124.0	1.35	365.1	0.54	0.60
	2	77.1	199.0	1.06	383.1	0.44	0.48
	3	80.2	220.3	0.98	363.8	0.41	0.44

earity of both the resistivity (at slightly higher T) as well as of $R_H^{-1}(T)$ might be associated to oxygen reordering in the CuO chains. Contrary to the 1:2:3 compound the inverse Hall coefficient of the 2:2:1:2 films can be nicely fitted to the above expression in the whole temperature range.

In *nonmagnetic* normal metals, more precisely such metals as can be described fairly well by the free-electron-gas model and that do not display any peculiarities in the scattering mechanism, the Hall number $n_H = (R_H e)^{-1}$ is a measure of the carrier concentration. However, due to the strong variation of the experimental R_H curves with temperature such a relationship is questionable. Note also the general remarks and the results on the normal-state Hall coefficient for a more complicated band structure in the preceding sections. Therefore, in order just to get some ideas about the carrier concentration in the 1:2:3 and 2:2:1:2 samples, which in the following is also needed for a comparison with theory, we determine the sheet-hole concentration per Cu-site $n_H^* = V_0/(mR_H e)$ at two temperatures (see Table I). Here V_0 denotes the volume of the unit cell and m is the number of CuO_2 planes per unit cell. The corresponding values are as follows: $V_0 = 178 \text{ \AA}^3$, $m = 2$ for 1:2:3 and $V_0 = 460 \text{ \AA}^3$, $m = 4$ for 2:2:1:2, respectively.

B. Comparison of experiment and theory

In the following the unusual temperature dependence of the Hall coefficient, which has been observed in the 1:2:3 and 2:2:1:2 films, is compared to the results of our calculations based on the renormalized tight-binding model. Before doing this, it should be emphasized that the simple dispersion (1) for the electronic band structure neither considers the quasi-one-dimensional CuO chains in $\text{YBa}_2\text{Cu}_3\text{O}_{7-x}$ nor any influence of the BiO_2 planes in $\text{Bi}_2\text{Sr}_2\text{CaCu}_2\text{O}_y$. The calculations of the Hall coefficient were done for fixed hopping parameters t and t^* varying the doping concentration δ . The latter is not reliably known for 1:2:3 and 2:2:1:2. For 1:2:3 ($T_c \approx 90\text{ K}$) the hole concentration δ has been chosen to be close to a sheet-hole concentration of 0.20–0.25 per Cu site, which Shafer *et al.*³⁷ found experimentally by iodometric titration. In the case of the 80 K 2:2:1:2 compound we have assumed similar values. For t we take such values, which lead to a reasonable bandwidth of $\approx 0.6 - 1.2\text{ eV}$. Then the next-nearest-neighbor term t^* has been chosen to fit the experimental data as well as possible. At this stage it should be noted that the corresponding bandwidths predicted by conventional band-structure calculations are, in general, significantly larger.⁸ The volume of the *model*

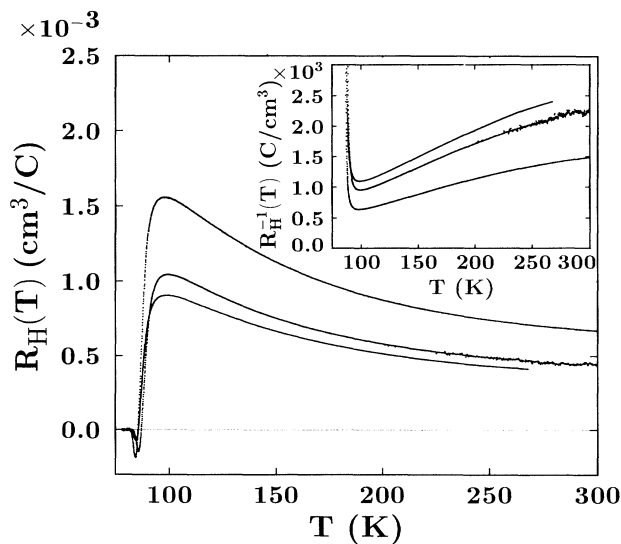


FIG. 6. Temperature dependence of the Hall coefficient of several 1:2:3 films for $B \parallel c$ direction ($B = 5\text{ T}$). The inset shows the inverse Hall coefficient $R_H^{-1}(T)$ vs temperature.

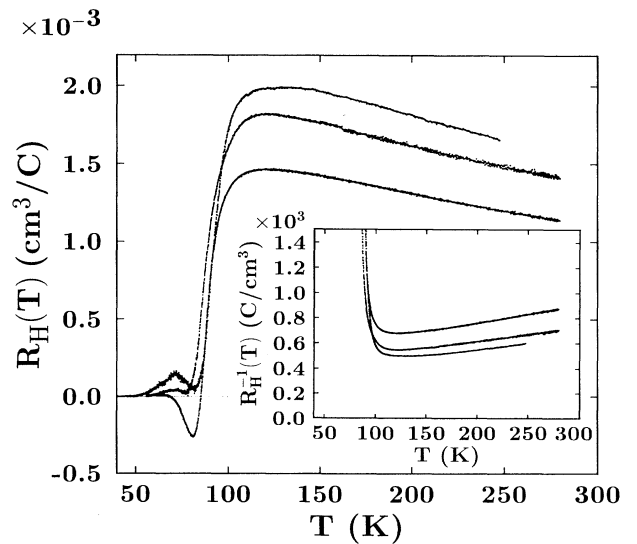


FIG. 7. Temperature dependence of the Hall coefficient of several 2:2:1:2 films for $B \parallel c$ direction ($B = 5\text{ T}$ for the upper curve, $B = 3\text{ T}$ for the two lower curves). The inset shows the inverse Hall coefficient $R_H^{-1}(T)$ vs temperature.

unit cell $\tilde{V}_0 = V_0/m$ entering in the calculations is 89 \AA^3 for 1:2:3 and 115 \AA^3 for 2:2:1:2, respectively. Figure 8 displays the data of the 1:2:3 samples as well as the theoretical curves for a certain choice of parameters.

Firstly, we concentrate on the results found for the k -dependent relaxation time τ_l assuming that excess holes are created close to the top of the $\text{O } 2p$ band. The evaluated Hall coefficients for $t = 0.40 \text{ eV}$ and $t^* = 0.175 \text{ eV}$ [the corresponding bandwidths $W = 8t\delta$ vary between 0.8 eV ($\delta = 0.25$) and 1.12 eV ($\delta = 0.35$)] are positive and of the correct magnitude. Moreover, similarly to the experimental data, the calculated R_H is also a strongly decreasing function of T , but concerning the detailed temperature dependence there are significant differences. The pronounced curvature of the experimental data is only qualitatively reproduced. For the same choice of parameters, but assuming a constant relaxation time τ_0 , the evaluated R_H curves (for clarity not shown here) are essentially *negative* in the same temperature range. Additionally shown in Fig. 8(a) is the Hall coefficient for τ_0 and a different choice of the parameters $t = 0.30 \text{ eV}$ and $t^* = 0.075 \text{ eV}$. $R_H(T)$ is also of the correct magni-

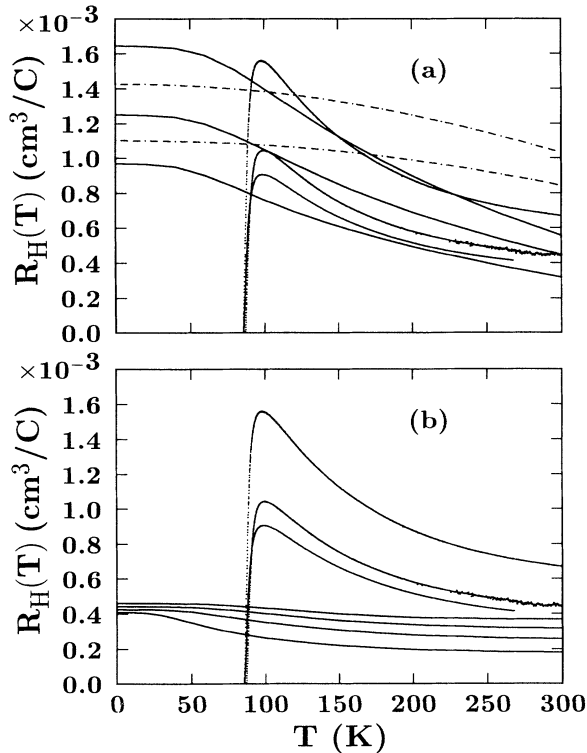


FIG. 8. Comparison between theory and experimental Hall coefficient of the 1:2:3 samples. (a) Doping creates holes in the $\text{O } 2p$ band. Solid lines are the predictions for the parameters $t = 0.40 \text{ eV}$, $t^* = 0.175 \text{ eV}$, and $\delta = 0.25, 0.3, 0.35$ (from top to bottom) assuming τ_l . The dot-dashed lines are the results for τ_0 and the parameters $t = 0.30 \text{ eV}$, $t^* = 0.075 \text{ eV}$, $\delta = 0.3$ (upper curve), and $\delta = 0.35$ (lower curve). (b) Doping creates holes in the antibonding CuO_2 band. Calculations for τ_l and the hopping terms $t = 0.40 \text{ eV}$, $t^* = -0.16 \text{ eV}$ and different doping concentrations $\delta = 0.2, 0.25, 0.3, 0.35$ (from top to bottom).

tude and a slightly decreasing function of temperature; however, note the *opposite* curvature of the graphs.

Next we turn to the temperature dependence of the predicted Hall coefficient for the case that holes are doped in the antibonding CuO_2 subband and the constant- l relaxation time τ_l [Fig. (8b)]. For the transfer terms $t = 0.40 \text{ eV}$ and $t^* = -0.016 \text{ eV}$ the Hall coefficient is first a decreasing function of T before it slightly increases at higher temperatures. But in comparison to the experiment the predicted R_H is too small in magnitude. The reason is, roughly speaking, due to the higher carrier concentration $(1 + \delta)$. Assuming τ_0 the predicted Hall coefficient (not shown here) is an increasing function of T and thus in strong contradiction to the experiment. In this context it should be emphasized that Hall effect measurements on c -axis oriented $\text{YBa}_2\text{Cu}_4\text{O}_{8+x}$ films³⁸ and single crystals³⁹ reveal a much lower value of the normal-state Hall coefficient opposed to the 1:2:3 system. In this compound a rapid decrease of R_H just above T_c is seen, while at higher temperatures, say for $T > 150 \text{ K}$, the Hall coefficient slightly increases. Quite remarkably, the overall behavior of these $R_H(T)$ curves is qualitatively reproduced by the ones with $\delta \approx 0.30 - 0.35$ in Fig. 8 (b). In order to provide a direct comparison of the Hall data of $\text{YBa}_2\text{Cu}_4\text{O}_{8+x}$ and the predictions one has to multiply the theoretical curves for $\text{YBa}_2\text{Cu}_3\text{O}_{7-x}$ by the factor 1.12 (the ratio of the corresponding volumes of the unit cells).

Figure 9 shows the Hall coefficients of the 2:2:1:2 films versus temperature as well as some theoretical curves. The calculations were performed for the parameters $t = 0.45 \text{ eV}$ and $t^* = 0.18 \text{ eV}$ (the bandwidths W range from 0.99 to 1.26 eV) assuming the constant- l relaxation time and that holes are doped at the top of the $\text{O } 2p$ band. In the following we present the results only for this sit-

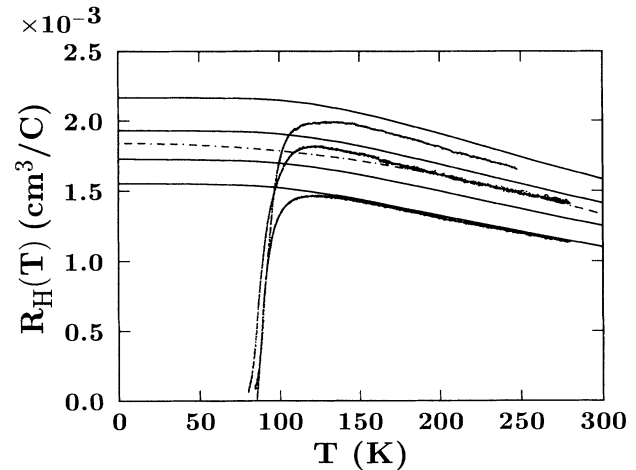


FIG. 9. Comparison between theory and experimental Hall coefficient of the 2:2:1:2 samples, assuming that holes are doped in the $\text{O } 2p$ band. The solid curves are the results for the parameters $t = 0.45 \text{ eV}$, $t^* = 0.18 \text{ eV}$, and $\delta = 0.275, 0.3, 0.325, 0.35$ (from top to bottom) assuming τ_l . The dot-dashed line is the result for $t = 0.3 \text{ eV}$, $t^* = 0.075 \text{ eV}$, and $\delta = 0.3$ taking τ_0 .

uation because doping in the antibonding CuO_2 band leads to predictions for the Hall coefficient, which are much smaller in magnitude than the experimental data. It can be clearly seen that the calculated normal-state Hall coefficients for the chosen parameters are in good quantitative agreement with experiment. This concerns the sign and the magnitude of R_H as well as its detailed temperature dependence. The fine tuning of $R_H(T)$ depends sensitively on the choice of the next-nearest hopping term t^* for fixed t . In order to achieve a good fit to the 2:2:1:2 data the particular choice of the renormalization factor in the energy dispersion (1) is not crucial. Taking the usual tight-binding model with *fixed* transfer terms, which of course are smaller than the above ones (say $t \approx 0.1 - 0.125$ eV, $t^* \approx 0.04$ eV) to retain the bandwidths of $W \approx 0.8 - 1.0$ eV, also provides a rather good agreement. It should be mentioned that the assumption of τ_0 and the choice of the parameters $t = 0.3$ eV, $t^* = 0.075$ eV, and $\delta \approx 0.3$ leads to a fairly good description of the Hall data. If one takes the fitted doping concentrations δ seriously—some objections will be discussed below—our study indicates that the experimentally determined values for n_H^* (Table I) are larger.

In the present study all calculations have been performed for the exact two-dimensional system. A more realistic model should also take into account a *small* interlayer coupling between adjacent CuO_2 planes (see also the discussion of the role of the interplane coupling on the DOS in a preceding chapter). This can be done, e.g., by introducing a transfer term t_z ($t_z \ll t$), which results in an energy dispersion along z direction.⁴⁰ It is commonly believed that a small interlayer coupling does not significantly influence the transport properties along the CuO_2 planes. Concerning our results on the Hall component $R_{xyz}^H(\delta, T)$, which have provided a qualitatively good fit to the experimental Hall data, we also believe that they would not be *significantly* altered. The reason is, as has already been mentioned, that the origin of the pronounced temperature dependence of R_H in our simple one-band model is due to the narrow bandwidths. Therefore also in the modified band-structures, which, in comparison to the original tight-binding bands, have slightly broader bandwidths, such areas of constant energies in the Brillouin zone with different curvatures still contribute to the Hall coefficient leading to a pronounced temperature dependence of it. In this context it is worth noting that calculations^{41,42} for the other Hall components R_{yzx}^H and R_{zxy}^H of the 1:2:3 compound predict a *negative* sign.

C. Fermi surfaces

If we restrict the discussion only to the strong temperature dependence of the Hall coefficient in the normal state of the 1:2:3 and 2:2:1:2 samples, it seems at first glance that the simple renormalized tight-binding model, assuming that holes are created close to the top of the effective oxygen band and the constant- l relaxation time, provides a rather good description. However, any model for the Hall effect in HTSC has to be consistent also with the observed Fermi surfaces (FS)

in the normal state. The existence and particularly the shape of the FS in HTSC [e.g., for $\text{YBa}_2\text{Cu}_3\text{O}_{6.9}$ (Ref. 5) and $\text{Bi}_2\text{Sr}_2\text{CaCu}_2\text{O}_y$ (Refs. 6 and 7)] has been clearly established by angle resolved photoemission spectroscopy. These experimental results indicate large FS satisfying Luttinger's theorem,⁴³ i.e., the Fermi surface volume contains $1 + \delta$ holes. Concerning this feature, there is a striking similarity between experimental data and the predictions of conventional band theory. The corresponding shapes of the Fermi surfaces of our model are shown in Figs. 10(a) and 10(b) for different parameters. Taking the same parameter set, which has provided a qualitatively good fit to the Hall data of the 1:2:3 films, the predicted small Fermi surfaces are in strong contradiction to the photoemission data. This is also true for the choice of parameters, which lead to a good fit to the Hall coefficient of the 2:2:1:2 compound. In the other case, assuming that additional holes accumulate in the CuO_2 subband, the overall shape of the Fermi surface seems to be in good agreement with photoemission experiments. However, as has been already pointed out, this picture would be incompatible with the Hall coefficient. A comprehensive discussion of this striking problem can be found in Ref. 44. It has been mentioned that doping in the antibonding CuO_2 band, assuming the constant- l relaxation time, may describe the observed Hall effect in the $\text{YBa}_2\text{Cu}_4\text{O}_{8+x}$ compound quite well. Furthermore, the corresponding large Fermi surface is also consistent with recent results of band-structure calculations.⁴⁵ Therefore,

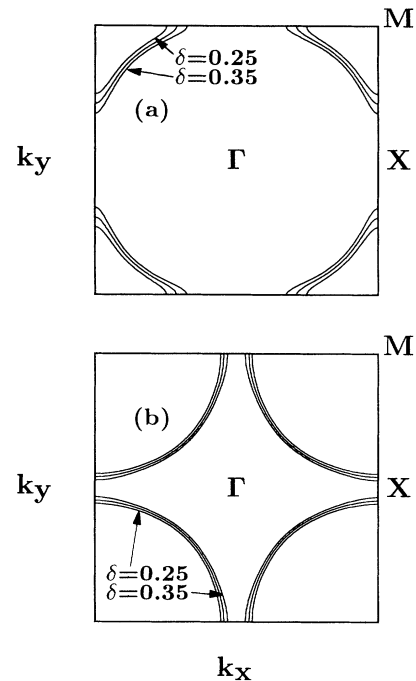


FIG. 10. Fermi surfaces for different hole doping concentrations δ . (a) Doping creates holes in the $\text{O}2p$ band. The parameters are $t = 0.40$ eV, $t^* = 0.175$ eV, and $\delta = 0.25, 0.3, 0.35$ (from outer to inner curve). (b) Doping creates holes in the CuO_2 band. The Fermi surfaces are plotted for $t = 0.40$ eV, $t^* = -0.16$ eV, and $\delta = 0.25, 0.3, 0.35$.

it would be very interesting to perform experiments (e.g., ARPES) on this system in order to reveal its electronic structure.

Concerning the unusual doping and temperature dependence of the Hall coefficient in the normal state of the p -doped HTSC several approaches have been suggested.⁴⁶ On the basis of conventional band-structure calculations,^{3,41,42} a simple tight-binding model,⁴⁰ which also considers the interplane coupling, and strongly correlated models^{4,14,47-52} some normal-state transport properties, including the Hall coefficient, have been investigated. It is worth noting that in some of the strongly correlated models,^{50,51} which consider the coupling of fermions to spinless bosons via a gauge field, a completely different origin (compared to our approach) of the unusual temperature dependence of the normal-state Hall coefficient has been suggested. This is also the case for the non-Fermi-liquid-based approach of Anderson.⁵² Here, in the two-dimensional Luttinger-liquid theory two quite different relaxation times, namely, a transport scattering rate τ_{tr} and a transverse (“Hall”) relaxation rate τ_{\perp} , have been introduced in order to correlate the anomalous in-plane resistivity and Hall coefficient. The predictions of this model for the Hall angle are in good agreement with data on both pure and doped single crystals (see, e.g., Ref. 53).

But so far, no satisfactory explanation of the doping *as well as* the temperature dependence of R_H in the normal state of the HTSC, which is, furthermore, also consistent with the large Luttinger Fermi surface, has been achieved.

D. Normal-state properties

For the sake of completeness we have calculated some other normal-state properties within our simple model taking those parameters, which have provided a rather good fit to the Hall data. We focus here only upon the density of states at the Fermi energy E_F , the Fermi velocity, the Drude plasma energy, and the effective mass defined by

$$N(E_F) = \frac{2}{N} \sum_{\mathbf{k}} \delta(\epsilon(\mathbf{k}) - E_F), \quad (9)$$

$$v_F = (\langle v_x^2 \rangle + \langle v_y^2 \rangle)^{1/2} = (2\langle v_x^2 \rangle)^{1/2}, \quad (10)$$

$$(\hbar\Omega_{p_{xx}})^2 = (\hbar\Omega_{p_{yy}})^2 = \frac{4\pi e^2 \hbar^2}{\tilde{V}_0} N(E_F) \langle v_x^2 \rangle, \quad (11)$$

$$m_{xx}^{-1} = m_{yy}^{-1} = \hbar^{-2} \langle \partial^2 E / \partial k_x^2 \rangle. \quad (12)$$

Here $\langle A \rangle$ ($A = v_x^2, \partial^2 E / \partial k_x^2$) denotes the Fermi surface average:

$$\langle A \rangle N(E_F) = \frac{2}{N} \sum_{\mathbf{k}} A(\mathbf{k}) \delta(\epsilon(\mathbf{k}) - E_F). \quad (13)$$

The obtained results are listed in Table II. It should be noted that typical values for the Drude plasma energy and the Fermi velocity are significantly smaller than those predicted by band-structure calculations, which is essentially due to the narrow bands. The effective mass of the carriers is in good agreement with such values found, e.g., in ARPES measurements.⁷

V. SUMMARY AND CONCLUSIONS

We have performed Hall effect measurements on several epitaxial $\text{YBa}_2\text{Cu}_3\text{O}_{7-x}$ and $\text{Bi}_2\text{Sr}_2\text{CaCu}_2\text{O}_y$ films. The Hall coefficient in the normal state is holelike and exhibits a strong temperature dependence. In contrast to $\text{Bi}_2\text{Sr}_2\text{CaCu}_2\text{O}_y$ the variation of $R_H(T)$ in $\text{YBa}_2\text{Cu}_3\text{O}_{7-x}$ is more pronounced. A significant deviation of the $R_H^{-1}(T)$ curves from linearity at higher temperatures has been observed in $\text{YBa}_2\text{Cu}_3\text{O}_{7-x}$. Within the framework of a simple renormalized two-dimensional tight-binding model on a square lattice, which takes into account also the next-nearest-neighbor hopping, the normal-state Hall coefficient has been calculated as function of doping concentration and temperature using the relaxation-time approximation. The calculations have been performed for two choices of the relaxation time $\tau(\mathbf{k})$, i.e., a constant relaxation time τ_0 and the constant- l relaxation time $\tau_l = l(T, \delta) / |v(\mathbf{k})|$. Strong correlation effects are accounted for by doping-dependent hopping terms leading to band-narrowing effects. The interpretation of the Hall effect was done for two quite different as-

TABLE II. Calculated band parameters for copper-oxide superconductors. The calculations have been performed for different theoretical approaches. m_e denotes the bare electron mass.

	$\text{YBa}_2\text{Cu}_3\text{O}_{7-x}$ ^a	$\text{Bi}_2\text{Sr}_2\text{CaCu}_2\text{O}_y$ ^b	$\text{YBa}_2\text{Cu}_4\text{O}_{8+x}$ ^c	Unit
$N(E_F)$	7.59	4.59	5.65	states/(eV cell) (both spins)
$R_{xyz}^H(\tau_0, T=0)$	-0.121	0.307	0.492	(10^{-3} cm ³ /C)
$R_{xyz}^H(\tau_l, T=0)$	1.254	1.732	0.480	(10^{-3} cm ³ /C)
$\hbar\Omega_{p_{xx}}$	0.794	0.850	1.42	(eV)
$\langle v_x^2 \rangle^{1/2}$	3.07	4.81	6.73	(10^6 cm/s)
m_{xx}/m_e	4.79	4.01	3.92	

^a $t = 0.40$ eV, $t^* = 0.175$ eV, and $\delta = 0.3$; doping in the O 2p band.

^b $t = 0.45$ eV, $t^* = 0.18$ eV, and $\delta = 0.325$; doping in the O 2p band.

^c $t = 0.40$ eV, $t^* = -0.16$ eV, and $\delta = 0.3$; doping in the antibonding CuO_2 band.

assumptions about the hole doping. One approach assumes that additionally doped holes are created in an effective oxygen band, while in the second they are doped into an antibonding CuO_2 subband. It has been shown that the next-nearest-neighbor hopping t^* as well as the choice of the relaxation time, strongly influence the predicted Hall coefficient. Depending on t/t^* the critical doping concentration δ_c , where the sign change of the Hall coefficient occurs, can be varied in a wide range. Concerning the predicted strong temperature dependence of R_H in our one-band model it should be stressed that it is only due to the Fermi distribution function. The origin is essentially attributed to the narrow bands of the order of 0.5–1.0 eV. In the case that doped holes are created in the effective oxygen band the theoretical results are in good quantitative agreement with the observed Hall coefficient of the $\text{Bi}_2\text{Sr}_2\text{CaCu}_2\text{O}_y$ samples for a reasonable choice of parameters. Assuming the constant- l relaxation time and that holes accumulate in the oxygen band also the strong temperature dependence of R_H of the $\text{YBa}_2\text{Cu}_3\text{O}_{7-x}$ films can be qualitatively reproduced. The estimated carrier concentration of both systems is $(2.8-3.9) \times 10^{21} \text{ cm}^{-3}$ for 1:2:3 and $(2.1-3.0) \times 10^{21} \text{ cm}^{-3}$ for 2:2:1:2, respectively. However, the predictions for the shape of the Fermi surfaces are not compatible with the large Luttinger Fermi surfaces observed by photoemission

experiments. These experimental Fermi surfaces seem to be compatible with the case that doping creates holes in the less than half-filled CuO_2 band, but as has been shown in our investigation there is no agreement with experimental Hall data. Here the theoretical Hall coefficient is much smaller than the experimental ones. This contradiction is a serious problem for our model. Quite remarkably, the predictions in the latter case seem to be consistent with the unusually small Hall coefficient observed in the $\text{YBa}_2\text{Cu}_4\text{O}_{8+x}$ compound. Moreover, the corresponding large Fermi surfaces are comparable to the predicted ones by band-structure calculations.

Finally, we have also calculated some band parameters for those transfer terms and doping concentrations, which have provided a good fit to the Hall data. Typical values are $(3-7) \times 10^6 \text{ cm/s}$ for the Fermi velocity, 0.8–1.4 eV for the Drude plasma energy, and $4-5 m_e$ for the effective carrier mass.

ACKNOWLEDGMENTS

One author (R.H.) wishes to thank D. Rainer and J. Heym, Universität Bayreuth, for many useful discussions and stimulating support. This work was supported by the Bundesministerium für Forschung und Technologie.

*Also at Siemens AG, Zentrale Forschung und Entwicklung, D-8520 Erlangen, Federal Republic of Germany.

¹N. P. Ong, in *Physical Properties of High- T_c Superconductors II*, edited by D. M. Ginzberg (World Scientific, Singapore, 1990), and references therein.

²S. Uchida, H. Takagi, H. Ishii, H. Eisaki, T. Yabe, S. Tajima, and S. Tanaka, *Jpn. J. Appl. Phys.* **26**, 440 (1987); N. P. Ong, Z. Z. Wang, J. Clayhold, J. M. Tarascon, L. H. Greene, and W. R. McKinnon, *Phys. Rev. B* **35**, 8807 (1987); M. Suzuki, *ibid.* **39**, 2312 (1989).

³P. B. Allen, W. E. Pickett, and H. Krakauer, *Phys. Rev. B* **36**, 3926 (1987).

⁴H. Fukuyama and Y. Hasegawa, *Physica B* **148**, 204 (1987).

⁵J. C. Campuzano, G. Jennings, M. Faiz, L. Beaulaigue, B. W. Veal, J. Z. Liu, A. P. Paulikas, K. Vandervoort, H. Claus, R. S. List, A. J. Arko, and R. J. Bartlett, *Phys. Rev. Lett.* **64**, 2308 (1990).

⁶T. Takahashi, H. Matsuyama, H. Katayama-Yoshida, Y. Otabe, S. Hosoya, K. Seki, H. Fujimoto, M. Sato, and H. Inokuchi, *Phys. Rev. B* **39**, 6636 (1989); C. G. Olson, R. Liu, D. W. Lynch, R. S. List, A. J. Arko, B. W. Veal, Y. C. Chang, P. Z. Jiang, and A. P. Paulikas, *ibid.* **42**, 381 (1990).

⁷G. Mante, R. Claessen, T. Buslaps, S. Harm, R. Mancke, M. Skibowski, and J. Fink, *Z. Phys B* **80**, 181 (1990).

⁸W. E. Pickett, *Rev. Mod. Phys.* **61**, 433 (1989), and references therein.

⁹P. W. Anderson, *Science* **235**, 1196 (1987).

¹⁰F. C. Zhang and T. M. Rice, *Phys. Rev. B* **37**, 3759 (1988).

¹¹V. J. Emery, *Phys. Rev. Lett.* **58**, 2794 (1987).

¹²G. Kotliar, P. A. Lee, and N. Read, *Physica C* **153-155**, 538 (1988); D. M. Newns, M. Rasolt, and P. Pattnaik, *Phys. Rev. B* **38**, 6513 (1988).

¹³G. Baskaran, Z. Zou, and P. W. Anderson, *Solid State Commun.* **63**, 973 (1987).

¹⁴H. Kaga, *Physica C* **172**, 400 (1991).

¹⁵J. Yu, S. Massidda, and A. J. Freeman, *Physica C* **152**, 273 (1988); R. S. Markiewicz, *J. Phys. Condens. Matter* **1**, 8911 (1989).

¹⁶J. Labbe and J. Bok, *Europhys. Lett.* **3**, 1225 (1987); I. E. Dzyaloshinskii, *Zh. Eksp. Teor. Fiz.* **93**, 1487 (1987).

¹⁷R. S. Markiewicz, *Physica C* **177**, 171 (1991).

¹⁸C. C. Tsuei, *Physica A* **168**, 238 (1990); D. M. Newns, P. C. Pattnaik, and C. C. Tsuei, *Phys. Rev. B* **43**, 3075 (1991).

¹⁹C. M. Varma, P. B. Littlewood, S. Schmitt-Rink, E. Abrahams, and A. E. Ruckenstein, *Phys. Rev. Lett.* **63**, 1996 (1989).

²⁰P. W. Anderson, *Phys. Rev. Lett.* **64**, 1839 (1990).

²¹K. Levin, Ju H. Kim, J. P. Lu, and Qimiao Si, *Physica C* **175**, 449 (1991).

²²J. M. Ziman, *Electrons and Phonons* (Oxford University Press, New York, 1960).

²³B. Roas, L. Schultz, and G. Endres, *Appl. Phys. Lett.* **53**, 1557 (1988).

²⁴P. Schmitt, L. Schultz, and G. Saemann-Ischenko, *Physica C* **168**, 475 (1990).

²⁵B. Roas, L. Schultz, and G. Saemann-Ischenko, *Phys. Rev. Lett.* **64**, 479 (1990).

²⁶P. Schmitt, P. Kummeth, L. Schultz, and G. Saemann-Ischenko, *Phys. Rev. Lett.* **67**, 267 (1991).

²⁷R. Hopfengärtner, M. Leghissa, G. Kreiselmeyer, P. Schmitt, B. Holzapfel, I. Khassanov, J. Ströbel, and G. Saemann-Ischenko, *Physica C* **185-189**, 1281 (1991).

²⁸B. Hensel, B. Roas, S. Henke, R. Hopfengärtner, M. Lipfert, J. P. Ströbel, M. Vildić, and G. Saemann-Ischenko,

- Phys. Rev. B **42**, 4135 (1990).
- ²⁹J. Schützmann, W. Ose, J. Keller, K. F. Renk, B. Roas, L. Schultz, and G. Saemann-Ischenko, *Europhys. Lett.* **8**, 679 (1989).
- ³⁰N. Klein, G. Müller, S. Orbach, H. Piel, H. Chaloupka, B. Roas, L. Schultz, U. Klein, and M. Peiniger, *Physica C* **162-164**, 1549 (1989).
- ³¹J. Dengler, G. Ritter, G. Saemann-Ischenko, B. Roas, L. Schultz, B. Molnar, D. L. Nagy, and I. S. Szücs, *Physica C* **162-164**, 1297 (1989).
- ³²R. Hopfengärtner, B. Hensel, and G. Saemann-Ischenko, *Phys. Rev. B* **44**, 741 (1991).
- ³³S. W. Tozer, A. W. Kleinsasser, T. Penney, D. Kaiser, and F. Holtzberg, *Phys. Rev. Lett.* **59**, 1768 (1987).
- ³⁴P. Chaudhari, R. T. Collins, P. Freitas, R. J. Gambino, J. R. Kirtley, R. H. Koch, R. B. Laibowitz, F. K. LeGoues, T. R. McGuire, T. Penney, Z. Schlesinger, and A. P. Segmüller, *Phys. Rev. B* **36**, 8903 (1987); H. L. Stormer, A. F. J. Levi, K. W. Baldwin, M. Anzlowar, and G. S. Boebinger, *ibid.* **38**, 2472 (1988).
- ³⁵Y. Iye, S. Nakamura, and T. Tamegai, *Physica C* **159**, 616 (1989); L. Forro and A. Hamzić, *Solid State Commun.* **71**, 1099 (1989); Y. Lu, Y. F. Yan, H. M. Duan, L. Lu, and L. Li, *Phys. Rev. B* **39**, 729 (1989); L. Forro, D. Mandrus, C. Kendziora, L. Mihaly, and R. Reeder, *Phys. Rev. B* **42**, 8704 (1990).
- ³⁶T. R. Chien, D. A. Brawner, Z. Z. Wang, and N. P. Ong, *Phys. Rev. B* **43**, 6242 (1991).
- ³⁷M. W. Shafer, T. Penney, B. L. Olson, R. L. Greene, and R. H. Koch, *Phys. Rev. B* **39**, 2914 (1989).
- ³⁸K. Char, M. Lee, R. W. Barton, A. F. Marshall, I. Bozovic, R. H. Hammond, M. R. Beasley, T. H. Geballe, A. Kapitulnik, and S. S. Laderman, *Phys. Rev. B* **38**, 834 (1988).
- ³⁹J. Schoenes, J. Karpinski, E. Kaldis, J. Keller, and P. de la Mora, *Physica C* **166**, 145 (1990).
- ⁴⁰T. Schneider and M. P. Sørensen, *Z. Phys. B* **81**, 3 (1990).
- ⁴¹P. B. Allen, W. E. Pickett, and H. Krakauer, *Phys. Rev. B* **37**, 7482 (1987).
- ⁴²S. Massidda, J. Yu, K. T. Park, and A. J. Freeman, *Physica C* **176**, 159 (1991).
- ⁴³J. M. Luttinger, *Phys. Rev.* **121**, 942 (1961).
- ⁴⁴P. A. Lee, in *High Temperature Superconductivity: Proceedings of the Los Alamos Symposium, 1989*, edited by K. S. Bedell *et al.* (Addison-Wesley, Redwood City, CA, 1990), pp. 96-122.
- ⁴⁵T. Oguchi, T. Sasaki, and K. Terakura, *Physica C* **172**, 277 (1990); J. Yu, K. T. Park, and A. J. Freeman, *Physica C* **172**, 467 (1991).
- ⁴⁶N. P. Ong, *Phys. Rev. B* **43**, 193 (1991); R. S. Markiewicz, *Physica C* **177**, 445 (1991).
- ⁴⁷Ju H. Kim, K. Levin, and A. Auerbach, *Phys. Rev. B* **39**, 11633 (1989).
- ⁴⁸D. M. Newns, P. C. Pattnaik, M. Rosolt, and D. A. Papaconstantopoulos, *Phys. Rev. B* **38**, 7033 (1988).
- ⁴⁹S. A. Trugman, *Phys. Rev. Lett.* **65**, 500 (1990).
- ⁵⁰N. Nagaosa and P. A. Lee, *Phys. Rev. Lett.* **64**, 2450 (1990).
- ⁵¹L. B. Ioffe and G. Kotliar, *Phys. Rev. B* **42**, 10348 (1990).
- ⁵²P. W. Anderson, *Phys. Rev. Lett.* **67**, 2092 (1991).
- ⁵³T. R. Chien, Z. Z. Wang, and N. P. Ong, *Phys. Rev. Lett.* **67**, 2088 (1991).